LCLSII-TN-16-02

LCLS-II BSY Dump Window and Beam Rastering*

J. Welch

February 3, 2016

Contents

Abstract

LCLS-II beam parameters include a combination of extremely low emittance and very high average power resulting in thermal and stress challenges for the aluminum dump window through which the beam must pass in the BSY Dump. Analytic estimates given here show that without rastering, at the maximum power of 250 kW, the stresses in the window are well above the fatigue limit. A 1 mm radius circular raster pattern can reduce thermal stresses by about a factor of 2 for a 50 μm rms beam and bring the estimated stresses in the BSY Dump window to the level of the fatigue limit.

*Work supported in part by the DOE Contract DE-AC02-76SF00515. This work was performed in support of the LCLS-II project at SLAC.

1 Introduction

A conceptual design review was held on November 9, 2015 that covered the LCLS-II High Power Dumps and Windows [1]. The committee recommended that the engineering basis for the BSY Dump window design get further in-depth study. Among the recommendations are five which concern the issues of fatigue, combined transient and steady-state stresses, material properties at elevated temperatures and under high radiation dose and possibly corrosive conditions, and the possibility of boiling at the the wet surface of the window.

The committee also recommended that we consider defocussing the beam as well as exploring whether the three high power dumps could be made with the same technology. Regarding the latter, the baseline design for the SXR and HXR dumps is an aluminum core slug that does not require a window. It is clear that such a dump technology would not be able to handle the 250 kW beam beam that is required in the BSY. So by implication we must consider using the baseline

BSY Dump technology for the undulator lines, and that includes water cooled windows. For this reason we have included results of calculations scaled for the SXR and HXR beam powers in the tables that follow.

Window experience at SLAC and elsewhere includes beams at high average power but with much larger beam sizes and/or rastering. In such cases the window materials are not exposed to the radiation dose levels that the LCLS-II windows could receive. Calculations by Ludovic [2] show that at full beam power the average absorbed power density in the BSY Dump window is close to $10^6\ W/cm^3$, which is equivalent to an astounding $3.7 \times 10^8\ Gy/s$. Rastering the beam on the window, even a small amount, can have the effect of spreading out the intense radiation and heat to the point where the dose rate and temperature rise are comparable with previous window experience. Without rastering we must simply hope the behavior of the aluminum under extreme irradiation is not much different than it is with about 100 to 1000 times less dose for which there is experience.

In this paper we first describe an analytic model and explore various predictions for the non-raster case. Then we discuss how rastering effects scale with frequency and distance, and we give estimates for the a particular choice of raster pattern and frequency. We also discuss raster implementation issues. In Appendix A we provide a summary of existing and planned high power dump windows, and using the model in this paper we estimate peak temperature and stresses for those cases.

2 Non-raster Model

Because the power deposition per unit volume in the window is essentially constant as a function of depth, an analytic model can account for essentially all the salient features of the resulting near steady-state temperature distribution. Furthermore, simple dimensional analysis arguments can be used to estimate the magnitude of transient heating cases as well as the mechanical stresses. This model and some representative estimates are described in the next sections. Higher accuracy and more detailed stress and transient diffusion estimates can be done with finite element codes [3].

2.1 Window

Following reference [3] the window is assumed to be a uniform circular flat plate made of aluminum whose material properties are given in Table 1. Cooling is provided by direct contact with flowing water on one side of the window. The other side of the window is in vacuum. A nominal thickness of 4.5 mm was chosen to reliably hold the difference in pressure between the water and the vacuum, but as we shall see, has little effect on the resulting temperatures or stresses. The beam is assumed to strike the center of the plate at normal incidence and deposit a small fraction of its power in the plate.

2.2 Beam Properties

Beam parameters used in the thermal analysis are given in Table 2. The BSY dump is required to absorb up to 250 kW of beam power, while the two undulator dumps are required to absorb up to 120 kW in continuous operation. We are mainly interested in the highest average power, smallest beamsize cases. Single bunch heating effects are quite modest due to the limit on the charge per bunch of 300 pC. At maximum beam power of 250 kW the repetition frequency can be as high as 929 kHz, in which case the charge per bunch is 67 pC, or it can be as low as 208 kHz for 300 pC bunches, assuming 4 GeV operation.

The beam size chosen for thermal analysis is a conservative estimate of the minimum that might occur during operation [4]. The nominal beta functions at the BSY dump are both around 800 m and the distance from the last focussing magnet is 325 m. A beam with the nominal normalized emittance of 1 μm at 4 GeV will have an rms size (x or y) of $\sqrt{800 \times 10^{-6}/\gamma} = 320\ \mu$m, where γ is the Lorentz factor for electrons at 4 GeV. While 50 μm used in the analysis is considerably less than then nominal size, a healthy degree of conservatism is needed here because beam size will change during tuning and optimization of the machine. It would take a beta functions of about 30 m to produce a 50 μm beam. The long distance from the last focussing quadrupole in

Table 1: Material properties assumed for the window [16].

Material	Alloy	Modulus	Expansion Coefficient	Yield Strength	Fatigue Strength	Ultimate Tensile Strength	Thermal Conductivity	Specific Heat	Density
		GPa	10^{-6}/C	MPa	MPa	MPa	W/m/C	J/g/C	g/cm^3
Aluminum	6061 T6	68.9	23.6	276	96.5	310	167	0.896	2.7

Table 2: Beam parameters used in analysis

Location	Power kW	Beam Size μm
BSY	250	50
HXR	120	50
SXR	120	50

Table 3: Nuclear properties assumed for the dump windows [15]

Material	dE/dz_{min}	Radiation Length X_0
	MeV $g^{-1}cm^2$	MeV $g\ cm^{-2}$
Aluminum	1.615	24.01

the BSY helps to avoid an unexpectedly small spot at the window or dump, but it does not prevent the possibility. In the case of the undulator dumps, the distance to the focussing quadrupoles is not large and it is relatively easy to make a small beam spot.

The beam current density profile $J(r)$ is assumed to follow

$$J(r) = \frac{I}{2\pi\sigma^2} e^{-r^2/2\sigma^2}$$

where I is the total beam current, r is the radial coordinate, and σ is the rms beam size.

2.3 Power Deposited

An aluminum window is the first material the beam sees before being absorbed in the dump. It is thin enough (a few millimeters of aluminum compared with the radiation length of 89 mm) that there is essentially no shower development. Though energy loss from bremsstrahlung is far higher than from ionization, such energy is not absorbed in the window because it is very penetrating and simply goes downstream leaving ionization losses as the only significant source of absorbed energy in the window. The power deposited in the window by the beam is then $I \times dE/dz \times \Delta z$ where I is the beam current, Δz is the thickness of the window in the beam direction and dE/dz is energy loss per unit distance due to ionization. As the energy loss is very small compared with the total energy, dE/dz is essentially constant. For electrons at 4 GeV, to a good approximation $dE/dz = dE/dz_{min}$, where dE/dz_{min} is the minimum ionizing energy loss. Values used in the calculations are given in Table 3. This estimate of deposited power was checked against a FLUKA generated estimate [2] and found to be essentially identical.

Examples of power absorbed in an aluminum window of stated thickness Δz are given in Table 4. Absorbed power is proportional to window thickness.

2.4 Thermal Diffusion

Heating in the window is generated from the energy deposited by the beam and is transient in nature. Between beam pulses, to some extent there is diffusion of the heat out of the heated zone. Eventually a more

Table 4: Maximum power absorbed in Dump windows.

Location	Power kW	Δz mm	Power Absorbed W
BSY	250	4.5	123
HXR	120	4.5	59
SXR	120	4.5	59

or less steady-state distribution builds up. The transient diffusion of heat in the absence of a source is governed by [5]

$$\frac{\partial T}{\partial t} = D\nabla^2 T$$

where T is the temperature, D is the thermal diffusivity constant and is equal to the thermal conductivity divided by the product of the density and specific heat, and t is time. Without solving this equation, we can establish a relationship between time and distance scales for the diffusion of heat. For small time interval Δt and over a small distance ΔL

$$\frac{\Delta T}{\Delta t} \sim D\frac{\Delta T}{\Delta L^2}$$

Dividing out ΔT and inverting we have the fundamental scaling relationship between time and spatial dimensions for the diffusion of heat

$$\Delta t \sim \frac{\Delta L^2}{D}$$

For a given spatial dimension ΔL, if the time interval of interest is much shorter than $\Delta L^2/D$, then diffusion does not take place. Conversely if time interval of interest is much longer than $\Delta L^2/D$ then the system will be near steady-state. We will use these results to choose rastering pattern sizes and frequencies. Some values of interest for ΔL and Δt for aluminum alloy are given in Table 5.

2.5 Steady-State Temperature

As a first approximation we calculate the steady-state temperature profile assuming there is no cooling by the water at the face of the window. Instead we assume there is only edge cooling at a radius R_2. The effect of the water cooling will be evaluated as a second approximation. We also assume that all the beam power is deposited at a radius equal to σ. This leads to a small overestimate for the peak temperature rise in the window. With these approximations the temperature rise from the edge cooling temperature $T(R_{edge})$ to the central temperature is

Table 5: Values of frequency, time, and distance where thermal diffusion is important in Aluminum alloy

Freq.	Δt	ΔL
kHz	μs	μm
1000	1	8
100	10	26
1	1000	263
1 Hz	1 s	8.3 mm

$$\Delta T_{max} = \frac{P}{2\pi K \Delta z} \cdot ln\frac{R_{edge}}{\sigma}$$

where P is the total power absorbed by the window, K is the thermal conductivity, and Δz is the thickness of the window. The temperature distribution is

$$\begin{aligned} T(r) &= T_{max}, & r < \sigma \\ &= \tfrac{P}{2\pi K \Delta z} \cdot ln\tfrac{R_{edge}}{r} + T(R_{edge}), & r > \sigma. \end{aligned}$$

Some values for the peak steady-state window temperature assuming edge cooling at 35 C and $R_{edge} =$ 1 cm are given in Table 6. Note that the temperature estimates are not very sensitive to the assumptions of the edge radius or of beam size, since the temperature rise depends only logarithmically on the ratio. For example, if the beam size is 300 μm instead of 50 μm assumed in the calculation — a factor of six increase —the BSY window temperature rise would go from 138 C to 91 C.

These results indicate that as a first approximation, assuming only edge cooling, the peak window

Table 6: Estimated maximum temperature and temperature rise in dump windows without rastering. Edge cooling is assumed.

Window	Power	ΔT	T_{max}
	kW	C	C
BSY Dump	250	138	173
HXR Dump	120	66	101
SXR Dump	120	66	101

surface temperature will be well above the water temperature. In fact, in the case of the BSY Dump window, assuming the water pressure is 70 psig, the saturation temperature is 158 C. As the estimated peak window temperature is 173 C boiling is a distinct possibility. Now we will turn to the question of heat transfer to the water and compare with edge cooling.

2.6 Heat Transfer to Water

In the preliminary window design water is directed at the window with a flow velocity of approximately 4 to 5 fps [3]. An effective hydraulic diameter is needed before a heat transfer coefficient can be calculated. If we use the diameter of water feed tube as the hydraulic diameter (turbulence at the window should be at least as high as turbulence in the tube) then the effective hydraulic diameter is 2 inches. With these assumptions the heat transfer coefficient h works out to about 5000 $Wm^2\ C^{-1}$. An effective cooled area required for the window heat to be transferred can be estimated from

$$P = \text{Effective cooled area} \times \text{h} \times \Delta\text{T}$$

where ΔT is the temperature difference between the aluminum surface and the water. For the BSY window this area works out to be 1.78 cm^2 and corresponds to an effective surface cooling radius R_{eff} of about 0.7 cm. This is not far from the edge cooling radius assumed of 1 cm assumed in the first approximation. A more detailed calculation that integrates the edge-cooled derived logarithmic temperature profile finds an effective radius for water cooling to be even closer to 1 cm.

The effect of the surface cooling by the water is to lower the radial heat flux in the window. Because the window thickness is about one-half of effective surface cooling radius the reduction in temperature distribution due to surface cooling is not large. In fact it should be less than the effect of making the edge cooled radius equal to the thickness, which is about a 10 C reduction in the peak temperature. These effects are illustrated schematically in Figure 1

2.7 Effect of Boiling

For the BSY Dump window the estimated peak temperature is somewhat above the saturation temperature so boiling is a possibility, particularly if the pressure is reduced below the 70 psig assumed. The effect of boiling would be to rapidly increase the heat transfer coefficient in the region of boiling, provided the heat flux does not get too high[1]. This keeps the wall temperature close to the saturation temperature for small radii. If the power is increased further the region of boiling increases. But because of the very rapid rise in the heat transfer coefficient with excess temperature, the wall temperature stays close to the saturation temperature over the entire region.

2.8 Stresses

Rough approximations to the levels of stress induced by the thermal changes in the window can be made assuming the heated material is completely confined by the much larger cooled adjacent material. This approximation overestimates the real stresses because the surrounding cool material will take up some of the thermally induced strain. A proper calculation with finite element methods is needed for accurate results. Nevertheless, given the uncertainties in material properties under the highly unusually conditions of extreme irradiation and temperature gradients, rough conservative approximations can be used as a guide.

[1]For nucleate boiling of water, Reference [6] shows roughly a factor of four increase in the heat flux for a 5 C increase in the difference between the wall temperature and the saturation temperature

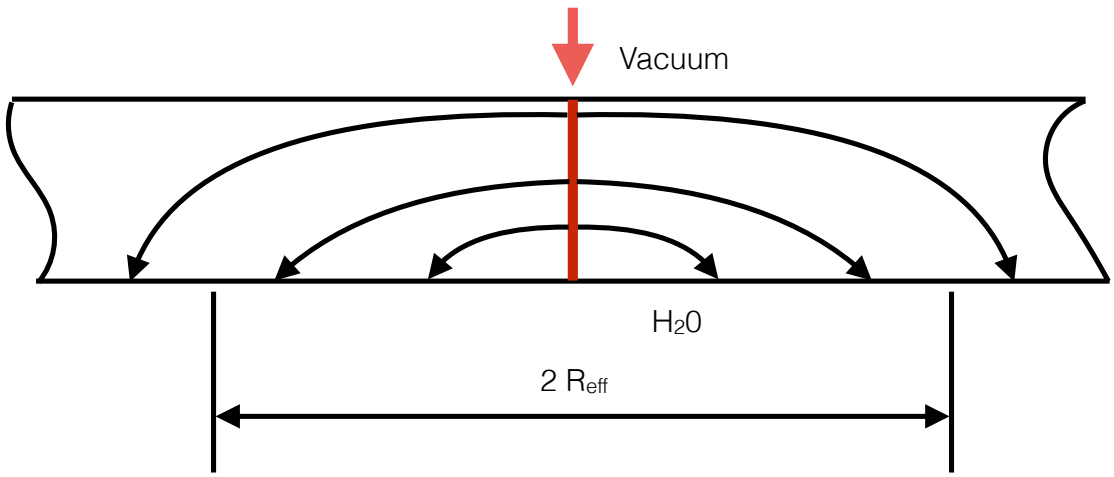

Figure 1: Illustration of the heat flow through a section of the aluminum window to the cooling water.

Normally when the temperature of a free body changes it will expand or contract with zero stress according to

$$\frac{\delta L}{L} = \alpha \Delta T$$

where L is the length of the body and α is the coefficient of thermal expansion. To completely confine the body to prevent its expansion when heated a mechanical stress is required from the surrounding material that is equal to $\alpha E \Delta T$, where E is the modulus of elasticity. We define $S = \alpha E \Delta T$ as the rough approximation of the thermal stresses involved and compare S with fatigue, yield, and ultimate stresses for the material in Table 7. In the BSY Dump case the estimated thermal stress is more than twice the fatigue stress and comparable with the yield stress. This brings into question the lifetime of the BSY Dump window. Scaled to the undulator beamline power limit of 120 kW, the estimated thermal stresses are comparable with the fatigue stress and more than a factor of two below the yield stress.

Table 7: Estimated peak induced thermal stress compared with fatigue and yield stresses for 6061 aluminum.

Window	Power	Thermal	Fatigue	Yield
	kW	MPa	MPa	MPa
BSY Dump	250	224	97	276
HXR Dump	120	107	97	276
SXR Dump	120	107	97	276

3 Rastering

Moving the beam spot on the window, even a small distance, can substantially reduce the steady-state temperatures induced. For simplicity we only consider a raster pattern where the beam is moving on a circle of radius R_{raster} and thus we maintain the cylindrical symmetry. To understand the effect of raster we first discuss the time and distance scales involved for thermal diffusion such that the rastered beam behaves thermally as if it is a uniformly distributed source. Next we report the results of the thermal calculations given the effectively larger source size. Finally we discuss implementation issues.

3.1 Time and Distance Scales

When rastering the beam on a circle there are two questions that have to answered: What is the radius and what is the frequency. A large radius will spread the heat out more but requires more aperture from the accelerator and more powerful magnets to deflect the beam. A high enough frequency will make the temperature distribution closer to the steady-state distribution but also requires more from the deflecting magnets. First we will deal with the radius choice.

The steady-state thermal model of a non-rastered beam assumed the current was a thin circular ring with a radius equal to the rms beam size. At high frequency rastering on a circle with radius much greater than the beam size will yield the same temperature profile as predicted in the steady-state model with the beam size replaced by the raster radius. Thus if we choose a 1 mm raster radius the peak temperature will decrease by a factor of 2.3 (depending somwhat on the effective cooling radius) compared with the $\sigma = 50$ μm case without rastering that was described already. Increasing the radius to 10 mm makes this factor 5.3 but is much harder to accommodate in the machine aperture. The point is that we only gain slowly once the raster radius is large compared with the beam size.

Once the radius is chosen, we can choose a frequency. There are two time scales which both must be considered:

1. The time it takes for heat to diffuse the distance of the raster radius must be small compared with the raster period.

2. The distance heat diffuses from a beam spot in the time between bunches must be small compared to the space between bunch impact points.

Regarding item 1, the heat flow in the window will resemble a uniform ring at radius R_{raster} if the rastering period is much less than the time it take for heat to diffuse a distance R_{raster}. Inversely that is,

$$f_{raster} >> 1/\Delta T \approx R_{raster}^2/D.$$

For example if $R_{rastser} = 1$ mm then for the aluminum window this implies the condition that $f_{raster} >> 69$ Hz.

Table 8: Possible rastering parameters.

R_{raster}	Cooling factor	f_{raster}	Pile-up factor
mm		1000	
0.5	1.8	1000	17
1	2.3	1000	9
2	3.3	1000	4

The second item constrains the frequency such that the frequency must be high enough that heat from subsequent beam pulses does not pile up. This is more restrictive than the first criteria because of the high bunch frequency possible with LCLS-II. Said another way, the beam impact point must move enough between pulses that the heat which diffuses from one pulse does not reach the heated area from the next pulse. This is shown schematically in Figure 2. In the time between bunches heat can diffuse a distance $\Delta L_B = \sqrt{D/f_B}$, where f_B is the bunch repetition frequency. Thus we require

$$\frac{\omega_{raster} R_{raster}}{f_B} >> \sigma + \Delta L_B,$$

where ω_{raster} is the angular frequency. This can be written as

$$f_{raster} >> f_B \cdot \frac{\sigma + \Delta L_B}{2\pi R_{raster}}$$

The number of bunches that fall within the diffusion distance in the time between bunches is defined as the "pile-up factor". The steady-state temperature profile is temporally increased by roughly the pile up factor multiplied by the single pulse heating temperature rise which is typically 1 C or less for LCLS-II parameters.

Possible values for raster radii and frequency and pile-up factors are given in Table 8. The cooling factor is the factor by which the non-rastered peak temperature is decrease if rastering is employed.

3.2 Temperatures and Stresses

Representative temperature and stresses are calculated for $R_{raster} = 1$ mm and a $F_{raster} = 1$ kHz are

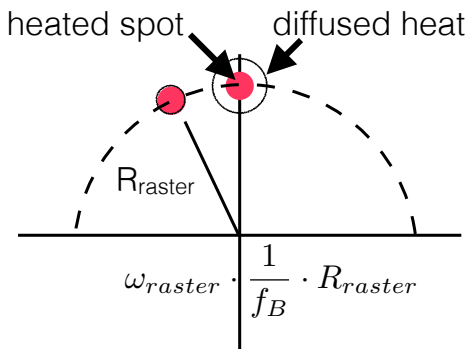

Figure 2: Raster frequency and diffusion of heat between bunches.

Table 9: Temperatures and stresses for R_{raster} = 1 mm and a f_{raster} = 1 kHz.

	Power	Temp.	Therm.	Fatigue	Yield
	kW	C	MPa	MPa	MPa
BSY	250	95	97	97	276
HXR	107	64	47	97	276
SXR	107	64	47	97	276

given in Table 9. In the BSY Dump window case the peak thermal stesses are equal to the fatigue limit stresses. Finite elements methods will be needed to see whether or not a more accurate calculation finds the peak stresses to be below the fatigue limits.

3.3 Implementation

If the rastering radius is kept to the level of 1 mm it will not require additional aperture. An allowance of 2 mm is given for steering and the raster motion can use part of this allowance. Air core corrector magnets and ceramic chambers would be required to produce the rastered beam. For a 1 mm deflection, depending on where the corrector magnets are place, the kick angle would be of order 30 μrad or less. For a 4 GeV beam this amounts to a peak integrated field strength of only 4 $G\ m$.

If implemented in the undulator dumps a rastered beam could affect the TCAV measurement and the FEL energy loss measurement. The XTCAV beam will kick the beam to an off-axis screen about 10 mm from the beam centerline. So a even 1 mm raster will not cause it to miss the screen. However, it will affect the image subtraction. Choosing a rastering frequency that is a harmonic of the XTCAV repetition rate would avoid this problem. Alternately the rastering motion can be measured or calculated and the image can be shifted to account for it. The energy loss measurement technique relies on measuring the difference between the pulse to pulse beam position and the position when there is no FEL energy loss. Once again the effect of the rastering can be measured or calculated and subtracted from the measured position.

4 Conclusion

For the BSY Dump window, rastering can provide a safety factor of 2 over the fatigue stress limit. For the undulator Dump windows, if they should be employed, rastering may or may not be useful. Finite element code calculations can be used to get a more accurate estimate of the safety factor for stresses. But unless rastering is employed we must simply hope the behavior of the aluminum under extreme irradiation is not much different than it was with about 100 to 1000 times less dose for which there is experience.

A Window Experience

High power electron beams have been, or will soon be, sent through windows at a few facilities. In all cases, because the beam size is relatively large or rastering is used, the peak temperature is expected to be lower than it would be for an un-rastered LCLS-II BSY Dump. Examples are discussed below.

A.1 SLAC

The SLAC SL-30 dump consist of a water cooled packed bed of aluminum spheres. It ran for about

8 days at 660 kW with a 1 mm beam size [17, 7]. Using the model in this paper the peak window temperature rise works out to be about 41 C and the peak thermal stress only about 0.7 of the fatigue stress limit. There would not be any boiling at the water window surface. So even though this window handled much more power than is required for the BSY Dump of LCLS-II, it was not subjected to as high stress or peak temperature as would be required when LCLS-II is running with maximum beam power at the minimum beam size.

A.2 CEBAF

CEBAF employs two 1 MW dumps, each with two 3 mm thick, edge-cooled, copper windows. They raster the beam in a 2 cm diameter circle at 60 cps to help prevent burn-through. With such rastering they estimate that with a 200 μA beam the average temperature in the window is 110 C [9]. Making the assumption of a 100 μm rms beam size, 35 C water inlet temperature, and a distance to edge cooling of 4 cm, the model employed in this paper predicts that without rastering the peak temperature rise would be over 800 C, but the rastering they use it brings the peak temperature down to 125 C — reasonably close to the CEBAF estimate of 110 C.

A.3 XFEL

The beam size is greater than 2 mm (x or y) on the XFEL dump window. The window is made of 10-15 mm thick graphite with a special coating. Only edge cooling is used. They predict the average temperature rise at a maximum train charge of 4 μC and 10 Hz is 30 C [8]. The material properties of the graphite window are not available, but assuming high conductivity graphite of 470 $W\ m^{-1}C^{-1}$ with a specific heat of 710 $J\ kg^{-1}C^{-1}$, and density of 2.21 $g\ cm^{-3}$ the model in this paper yields an average temperature rise of 20 C for the XFEL beam running at 10 Hz and 4 μC per burst— without rastering. Assuming a 15 mm thick window the maximum power deposited in the window is 230 W, which is considerable, but because of the excellent thermal conductivity and thickness, it does not lead to excessive temperature rise. The XFEL baseline design assumes a slow rastering (slow compared with 1 kHz) to reduce the peak temperature and stresses in the dump absorber, but the window would not require it.

A.4 TTF2

At the TTF2 the beam size on the window is greater than 1 mm and beam power can go up to 130 kW. It appears that the window is Ti [11] and they employ rastering with 4 cm diameter pattern at 1 kHz [12]. Assuming a beam to cooling edge distance of 8 cm and 1.5 mm window thickness, the model used in this paper indicates the peak temperature rise with rastering is about 360 C and the peak thermal stress is about 0.7 of the fatigue limit.

References

[1] LCLS-II BSY Beam Dump Design, Preliminary Design Review, November 9 11, 2015

[2] N. Ludovic, email 12/16/15.

[3] A. Ibrahimov, talk "LCLS-II BSY Beam Dump Design - PDR", Nov. 9-11, 2015

[4] T. Raubenheimer, 'High Power Dump Physics Requirements', talk given at the LCLS-II BSY Beam Dump Design, Preliminary Design Review, November 9 11, 2015

[5] F. Kreith, 'Principles of Heat Transfer', 2nd edition, International Textbook Co. Scranton Penn. p76 ff.

[6] W. Rohsenow 'A New Correlation of Pool-Boiling DataIncluding the Effect of Heating Surface Characteristics, Journal of Heat Transfer, May 1969, p245.

[7] SLAC-PUB-555

[8] "The European X-Ray Free-Electron Laser Technical design report", DESY 2006-097, edited by M. Altarelli et. al., p137-138 July 2007

[9] M. Wiseman, et. al., 'HIGH POWER ELECTRON BEAM DUMPS AT CEBAF', 17th Particle Accelerator Conference, Vancouver, Canada, 12 - 16 May 1997, pp.3761

[10] M. Maslov, et. al., 'Layout Considerations on the 25GeV / 300kW Beam Dump of the XFEL Project', DESY, August 2006, TESLA-FEL 2006-05

[11] S, Schreiber, 'FLASH The Free-Electron Laser User Facility Performance and operational issues Upgrade', talk given at PITZ Collaboration Meeting HZB, Berlin, 23-24 June 20

[12] M. Maslov, et. al., 'Design of a Beam Dump for the TTF-FEL Phase II (TTF2) Project'

[13] Xianghong Liu, et. al. 'A high average power beam dump for an electron accelerator', Nuclear Instruments and Methods in Physics Research A 709 (2013) 3743

[14] http://pdg.lbl.gov/2015/reviews/rpp2014-rev-atomic-nuclear-prop.pdf [15]

[15] K. A. Olive *et al.* [Particle Data Group Collaboration], Chin. Phys. C **38**, 090001 (2014).

[16] http://asm.matweb.com

[17] D. Walz memo to J. Welch, RP-RPG-131114-MEM-01, 11/14/2013, states SL-30 was run for about 8 days at 660 kW with a 1 mm beam size. with 1 mm rms spot size.